Volume 16
Number 41
7 November 2025
Pages 18961–19470

Chemical Science

rsc.li/chemical-science

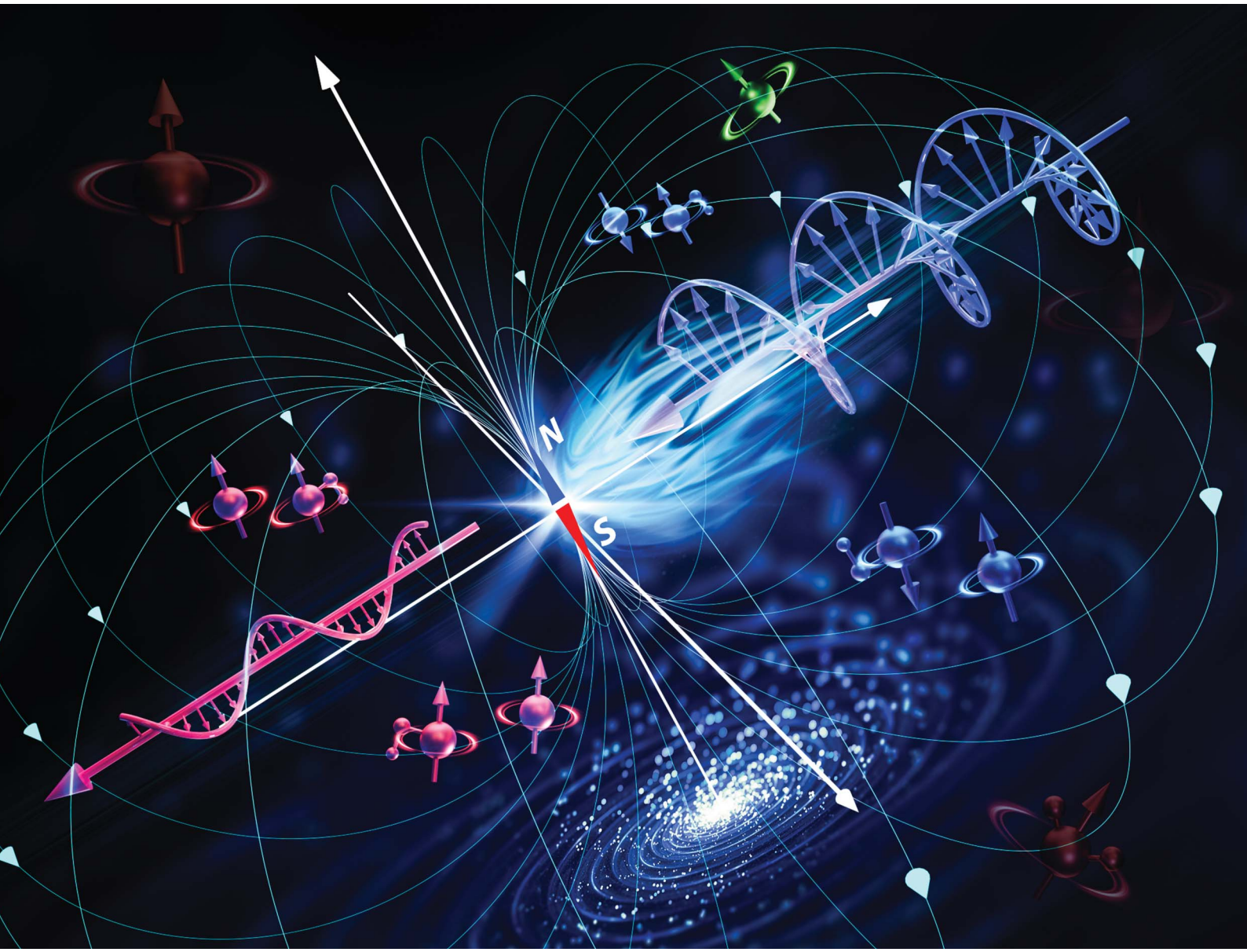

ISSN 2041-6539

ROYAL SOCIETY OF CHEMISTRY

EDGE ARTICLE
Zi-Shu Yang, Jun-Long Zhang *et al.*
Amplification of magnetic field effects *via* critical dynamics in a nonlinear oscillatory system

15 YEARS ANNIVERSARY

Chemical Science

ROYAL SOCIETY OF CHEMISTRY

EDGE ARTICLE

View Article Online
View Journal | View Issue

Check for updates

Cite this: *Chem. Sci.*, 2025, **16**, 19110

All publication charges for this article have been paid for by the Royal Society of Chemistry

Received 6th August 2025
Accepted 7th September 2025

DOI: 10.1039/d5sc05941k

rsc.li/chemical-science

Amplification of magnetic field effects *via* critical dynamics in a nonlinear oscillatory system

Shaojun Zhang,[a] Zi-Shu Yang,*[a] Bing-Wu Wang,[a] Song Gao [ab] and Jun-Long Zhang *[a]

Weak magnetic fields are known to modulate circadian rhythms in living systems, yet the chemical basis of their influence on oscillatory dynamics remains unresolved. This is a paradox given the negligible energies of the magnetic interactions ($\sim 10^{-2}$ kJ mol^{-1} T^{-1}) relative to thermal noise. Using the Briggs–Rauscher reaction as a model system, we show that applied magnetic fields (0–200 mT) induce an unprecedented amplification of oscillatory behavior *via* critical dynamics close to a Hopf bifurcation, driving 12% enhancement in reaction rate while 1500% enhancement in oscillation amplitudes of key intermediates (Mn^{2+} and I^-). Simulations using the de Kepper–Epstein model for the inherent non-linearity of feedback-driven oscillations reveal that magnetic field effects perturb bifurcation thresholds, magnifying even subtle changes in spin-selective radical recombination rates. Our findings establish a mechanism for magnetic field modulation in oscillatory networks, resolving the energy paradox and positioning magnetic fields as a potent tool for manipulating non-equilibrium chemical and biological systems.

Open Access Article. Published on 08 September 2025. Downloaded on 06.02.26 19:00:58.
This article is licensed under a Creative Commons Attribution-NonCommercial 3.0 Unported Licence.

Introduction

The influence of weak magnetic fields (~millitesla) (MFs) on circadian rhythms has been well-documented across various organisms,[1–4] from unicellular to multicellular; however, the underlying mechanism is not well understood. This knowledge gap primarily arises from the fact that the energies involved ($\sim 10^{-2}$ kJ mol^{-1} T^{-1}) are much smaller than the thermal energy (~2.5 kJ mol^{-1} at 300 K), leading to speculation that any magnetic field effect (MFE) should be too minor to be significant for most chemical reactions.[5–7] Biological rhythms are mainly regulated by the oscillation of chemical concentrations within a reaction network characterized by intricate positive and negative feedback loops.[8,9] Since the discovery of chemical oscillators by Belousov and Zhabotinsky (BZ), nearly 200 other chemical reactions that display periodic behavior have been identified, contributing to the understanding of circadian rhythms.[8,10–12] Therefore, investigating the effects of MFs—particularly their amplification by chemical oscillators—holds the promise of exploiting MFs as a means to influence chemical reactions with potential applications in chemistry, medicine, and materials science.[13–16]

Despite ongoing controversy, it is generally believed that the origin of MFEs lies in the spin-conserving nature of the recombination reactions of radical pairs (RPs), as exemplified by the light-dependent magnetic compass sense of migratory birds.[17,18] Nevertheless, MF-induced changes in reaction rates are small, even for millitesla field strengths.[17,19,20] This raises the question of whether such minor changes in individual reactions could accumulate to significantly alter oscillating systems, affecting downstream product concentrations or overall reaction rates. In 1996, Eichwald and Walleczek proposed the possibility of MFEs in enzyme kinetics when a reaction step involves RP intermediates.[21] Møller and Olsen demonstrated MFEs in the NADH peroxidase-oxidase system.[6,22] Beyond enzymatic reactions, MFs have also been shown to influence wave propagation in a cobalt(II)-hydrogen peroxide system and the BZ reaction, which is analogous to the biological tricarboxylic acid cycle.[23–29] Evidently, MFs could serve as a non-invasive means to regulate oscillations across diverse contexts, from laboratory settings to biological processes.

In contrast, the amplification of MFEs in biological or chemical oscillations has been largely neglected. Chemical oscillations feature complex feedback loops with non-linear and time-delay characteristics. Player *et al.* used the Brusselator model to demonstrate that even a minor MF-induced change in the rate constants of individual reaction steps could significantly influence the emergence or disappearance of periodic patterns in the concentrations of reaction intermediates, thereby altering oscillatory behavior.[30] The Hopf bifurcation, a key element in this process, shifts the system's steady state and mediates the transition between different oscillatory regimes.[31–34] Inspired by these findings, we monitored the periodic fluctuations in the concentrations of reaction

[a]*Beijing National Laboratory for Molecular Sciences, College of Chemistry and Molecular Engineering, Peking University, Beijing 100871, China. E-mail: zhangjunlong@pku.edu.cn; zsyang04@pku.edu.cn*

[b]*Guangdong Basic Research Center of Excellence for Functional Molecular Engineering, School of Chemistry and Chemical Engineering, Sun Yat-sen University, Guangzhou 510275, China*

© 2025 The Author(s). Published by the Royal Society of Chemistry

Open Access Article. Published on 08 September 2025. Downloaded on 06.02.26 19:00:58.
This article is licensed under a Creative Commons Attribution-NonCommercial 3.0 Unported Licence.

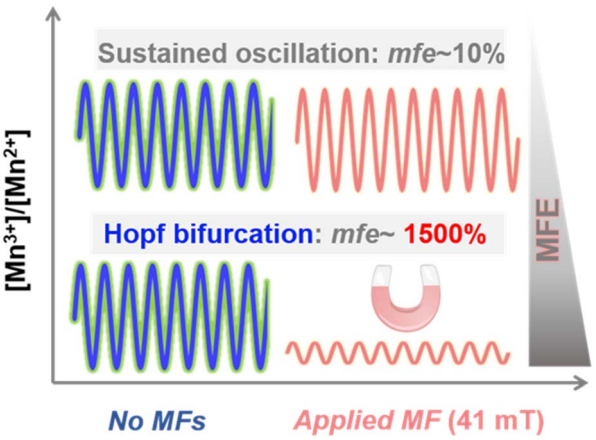

Scheme 1 Illustration of magnetic fields impacting a chemical oscillation reaction with magnetic field effects up to 1500% at a Hopf bifurcation.

intermediates and investigated how MFs affect rate constants and oscillation frequencies near the Hopf bifurcation.[32,35,36]

Here, we chose the Briggs–Rauscher (BR) reaction as a model system, catalyzed by Mn^{2+} ions in acidic solution, involving the oxidation of malonic acid ($CH_2(COOH)_2$ or **MA**; $C_3H_4O_4$), hydrogen peroxide (H_2O_2), and potassium iodate (KIO_3).[11,37,38] Unlike the classic BZ reaction, the BR reaction exhibits more pronounced color changes when starch is added, due to the formation of iodine, which causes the solution to oscillate between colorless, amber, and deep blue. Applying MFs (0–200 mT) revealed chemical amplification of MFEs near the Hopf bifurcation, enhancing intermediate signals by over an order of magnitude (Scheme 1). Simulations using the de Kepper–Epstein model show that minor changes in the autocatalysis step rate involving iodinated radical pairs at the Hopf bifurcation edge can significantly vary MFEs, supporting the observed amplification. This study offers new insights into how MFs influence circadian rhythms at the molecular level and their potential as an external field comparable to light and electricity in driving chemical reactions.

Results and discussion

Magnetic field effects on BR oscillations

The overall reaction of the BR oscillator (eqn (1)), can be divided into two component reactions, each consisting of multiple individual steps. The first involves Mn^{2+} ions and $IO_2^{\bullet}$ radicals and drives the conversion of iodate and hydrogen peroxide into iodine and oxygen (eqn (2)). The second is a non-radical process characterized by the slow consumption of free iodine by **MA** (eqn (3)).

$$CH_2(COOH)_2 + H^+ + IO_3^- + 2H_2O_2 \rightarrow ICH(COOH)_2 + 3H_2O + 2O_2 \quad (1)$$

$$2IO_3^- + 5H_2O_2 + 2H^+ \xrightarrow{Mn^{2+}} I_2 + 5O_2 + 6H_2O \quad (2)$$

$$5CH_2(COOH)_2 + H^+ + IO_3^- + 2I_2 \rightarrow 5ICH(COOH)_2 + 3H_2O \quad (3)$$

To investigate the magnetic sensitivity of the oscillations, we conducted experiments in MFs between 0 and 200 mT in a water bath at 21 °C, with initial concentrations: $[H_2O_2] = 1.3$ M, $[MnSO_4] = 0.0067$ M $[MA], = 0.067$ M, $[KIO_3] = 0.067$ M, $[H_2SO_4] = 0.1$ M. MFs were generated by a superconducting solenoid (Fig. S1) and the reactions were carried out in a cell displaced horizontally by 50 cm from its centre, ensuring a uniform vertical field (Fig. 1a). Fig. 1b illustrated the potentiometric monitoring of a glassy carbon electrode against an Ag/AgCl reference electrode. Distinct oscillations in the range 0.67–0.79 V was observed in 150 s, arising from periodic redox transitions in the reaction system. To quantify the timing and the MFE, we define τ_8 as the time required for the first 8 periods of the oscillation (SI, Section 3), and *mfe* as 100% × $[k_{obs}(B) - k_{obs}(B)]/k_{obs}(B)$. $k_{obs}(B)$ is the apparent rate constant in the presence of a MF with flux density B, and $k_{obs}(B) \propto \tau_8$. As shown in Fig. 1c, *mfe* decreased as the applied MFs was increased from 0 to 41 mT, reaching a minimum of −11.7% at 41 mT. Further increase in B from 41 to 200 mT, caused *mfe* to recover to −3.0% (Fig. S2). To rule out the magnetic-electrical interference, control experiments in peroxide-free solutions were carried out under these conditions: (i) at zero field, (ii) with applied MF (200 mT), and (iii) with switched fields. The potential traces exhibited slightly decrease and no oscillations throughout 400 s monitoring, with negligible abrupt observed with applied MF (Fig. S3). The results indicate that the observed MFEs originate from the response of the BR reaction to MFs.

To validate these results, we introduced starch as an indicator to allow the I_2 concentration to be monitored: from colorless (low $[I_2]$) *via* brown-yellow to blue (high $[I_2]$) and back. Using a video recorder to track the oscillations, τ_8 was measured as 112 s at 0 mT, increasing to 123 s at 41 mT (Fig. 1d, Supplementary Movie), yielding *mfe* = −9.8%. Fig. 1d indicates that τ_8 is increased by the application of a 41 mT MF. The period difference is defined by $\Delta\tau_n = \tau_n(41\text{ mT}) - \tau_n(0)$. As the number of oscillations (n) increased, $\Delta\tau_n$ steadily grew, reaching 11 s by the ninth cycle ($n = 8$, Fig. 1e).

We then attempted to compare MFEs on the iodination of malonic acid (eqn (3)) with those on the reaction intermediate I_2, representing thermodynamic and kinetic aspects of the reaction, respectively. Due to the difficulty of distinguishing **MA** from the product, $ICH(COOH)_2$, by high-performance liquid chromatography (HPLC), we employed benzyl malonic acid (**BzMA**) instead (Fig. S4 and S5).[39] After separating the reaction mixture with HPLC, we obtained a time-course plot for the conversion of **BzMA** at 0, 41, and 100 mT (Fig. 2a). The results indicate that while MFs had a minimal influence on the final yield of iodo-**BzMA** after 2000 s, they significantly affected the reaction rate, particularly during the initial stages. Specifically, the conversion at 300 s showed a decrease of 21% and an increase of 16% for 41 and 100 mT MFs, respectively. Additionally, we monitored the changes in $[I_2]$ by absorption at 460 nm for MFs of 0, 41, and 100 mT, as depicted in Fig. 2b. The time taken for the first five oscillations at 41 mT was 16% longer (70 s) than the value (60 s) observed at

Open Access Article. Published on 08 September 2025. Downloaded on 06.02.26 19:00:58.
This article is licensed under a Creative Commons Attribution-NonCommercial 3.0 Unported Licence.

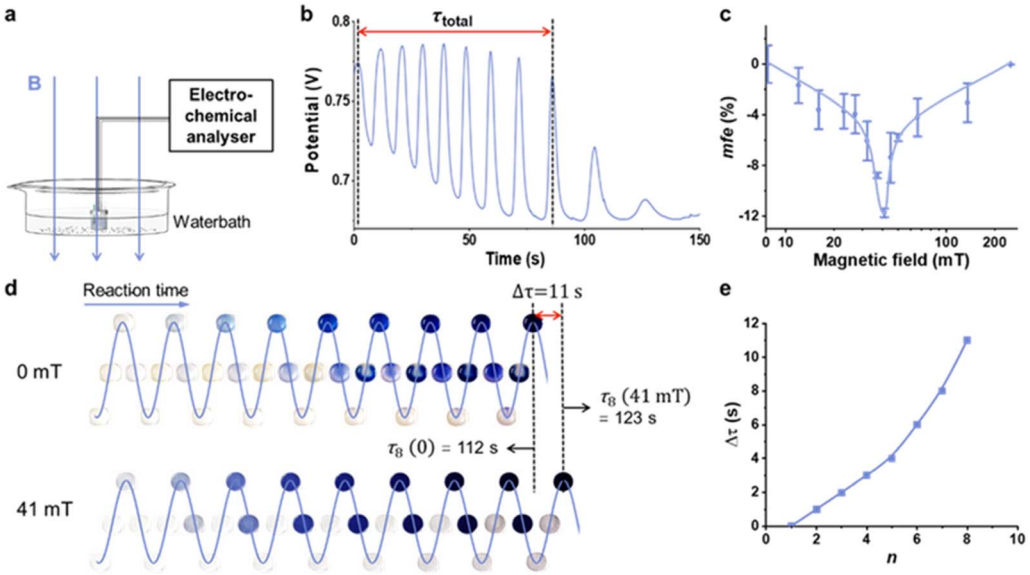

Fig. 1 Experimental setting and MFEs on BR oscillation. (a) The sample cell (1 × 1 × 1 cm) was placed 0.5 m from the centre of the magnet. (b) Potential *versus* time plot. (c) Relative k_{obs} of the BR reaction as a function of applied MF, the error bars represent the standard deviations of 3 independent measurements. (d) Images of the BR oscillation at 0 mT and 41 mT recorded by video. (e) The period difference between 41 mT and 0 mT varies with the oscillation number (*n*).

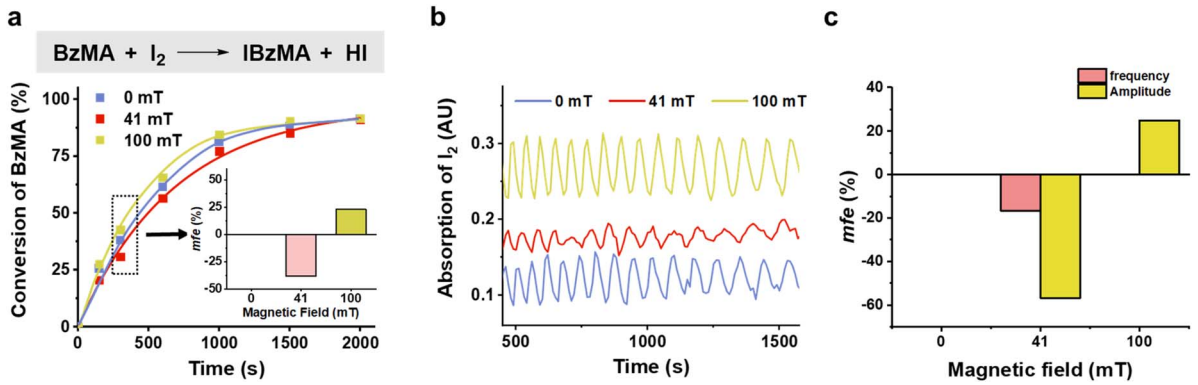

Fig. 2 MFEs on the conversion of **BzMA**. (a) Time trace of the **BzMA** conversion measured by HPLC at 0 mT (blue line), 41 mT (red line), and 100 mT (green line). (b) Time trace of I_2 absorbance (460 nm) in **BzMA** oscillating systems at 0, 41, and 100 mT. (c) Comparison of *mfe* between frequency and amplitude in Fig. 2b.

both 0 and 100 mT. Moreover, the amplitude of $[I_2]$ oscillation at 41 mT (0.026 absorbance units, a.u.) was smaller than that at 0 mT (0.060 a.u.) and at 100 mT (0.075 a.u). In summary, MFs have a more pronounced effect on the concentrations of intermediates (*e.g.*, I_2, with a reduction of 57% at 41 mT) than the final conversion of **BzMA** (approximately 0% at 41 mT), suggesting that **MFs** primarily modulate reaction kinetics (*e.g.*, altering intermediate formation rates) rather than affecting the thermodynamic equilibrium governing the final product yield.

Amplification of magnetic field effects at the hopf bifurcation

Theoretical models suggest that large MFEs on chemical oscillations might originate near a Hopf bifurcation[30,32,40] at which the amplitudes of limit-cycle oscillations are extraordinarily sensitive to small changes in reaction rate constants.[41] This possibility led us to investigate the Hopf bifurcation in the BR oscillator. Based on de Kepper–Epstein's model, we simplified the BR reaction into six steps (eqn (M1)–(M6)) and integrated the kinetics to obtain the time-dependence of the oscillations:

$$A + V + 2H \xrightarrow{k_1} U + P \quad (M1)$$

$$U + V + H \xrightarrow{k_2} 2P \quad (M2)$$

$$B + U \xrightarrow{k_3} 2U + Z + W(\text{Autocatalytic step}) \quad (M3)$$

$$2U \xrightarrow{k_4} P + A \quad (M4)$$

$$Z + M \xrightarrow{k_5} V \quad (M5)$$

$$W(aq) \xrightarrow{k_6} W(g) \quad (M6)$$

© 2025 The Author(s). Published by the Royal Society of Chemistry

Open Access Article. Published on 08 September 2025. Downloaded on 06.02.26 19:00:58.
This article is licensed under a Creative Commons Attribution-NonCommercial 3.0 Unported Licence.

where A = IO_3^-; B = H_2O_2; H = H^+; M = MA; P = HIO; U = HIO_2; V = I^-; W = O_2; Z = I_2, and k_{1-6} are rate constants.

Mn^{2+} ion plays a crucial role in the autocatalytic step, eqn (M3), which includes three reactions, eqn (4)–(6):

$$HIO_2 + IO_2^- + H^+ \rightarrow 2IO_2^{\bullet} + H_2O, \quad (9)$$

$$H_2O + Mn^{2+} + IO_2^{\bullet} \rightarrow HIO_2 + Mn(OH)^{2+} \quad (10)$$

$$2Mn(OH)^{2+} + H_2O_2 \rightarrow 2Mn^{2+} + O_2(aq) + 2H_2O \quad (11)$$

Therefore, we use the $[Mn^{3+}]/[Mn^{2+}]$ ratio to characterize the oscillatory behaviors. As established in prior study,[39] the glassy carbon electrode measures a mixed potential influenced by the concentrations of Mn^{3+} and iodide ions. At the constant iodide concentration ($[I^-]$), the fluctuations were directly linked to variations in the $[Mn^{3+}]/[Mn^{2+}]$ ratio. We directly quantified using an iodide-selective electrode, and confirmed a small variation within 10^{-9}–10^{-8} M (Fig. 5), demonstrating that the contribution of I^- to potential was negligible. The dominance of Mn redox species was further verified by cyclic voltammetry of Mn^{2+} under identical conditions ($E_{1/2}$ = 0.89 V, Fig. S6), showing significant overlap with the oscillation window according to Nernst equation.

By varying the initial concentration of Mn^{2+}, denoted as $[Mn^{2+}]_0$, the rate constant k_3 can be changed. This, in turn, enables us to pinpoint the location of the Hopf bifurcation. When $[Mn^{2+}]_0$ exceeded 8.89 mM, the oscillations stopped abruptly (Fig. S7a). Within the range from 2.78 to 6.67 mM, the amplitudes of the oscillations varied from 55 to 100 (Fig. 3b, with $[Mn^{2+}]_0$ = 6.67 mM normalized to 100). As $[Mn^{2+}]_0$ approached 2.78 mM, the amplitude becomes highly sensitive to small changes in concentration (Fig. 3a). For example, reducing $[Mn^{2+}]_0$ to 2.70 mM caused a dramatic decrease in the oscillation amplitude which dropped by approximately a factor of 11 from 56 to 5 (Fig. 3a and b). The oscillations disappear when $[Mn^{2+}]_0$ fell below 1.11 mM (Fig. S7a).

We attempted to fit the curve of the square of the oscillation amplitude (A^2) *versus* ($[Mn^{2+}]_0 - [Mn^{2+}]_{0,c}$) within the critical region (2.78–3.30 mM), where $[Mn^{2+}]_{0,c}$ represents the critical concentration as 2.78 mM (Fig. 3c). The resulting relationship was highly linear (R^2 = 0.997), indicating the bifurcation at $[Mn^{2+}]_0$ = 2.78 mM indicates a supercritical bifurcation. Further, the oscillation frequency showed a continuous decrease when $[Mn^{2+}]_0$ > 2.78 mM (Fig. S7b). Although the system evolves transiently due to reactant consumption, the observed results identifies the underlying bifurcation topology as a supercritical Hopf bifurcation. To better describe this

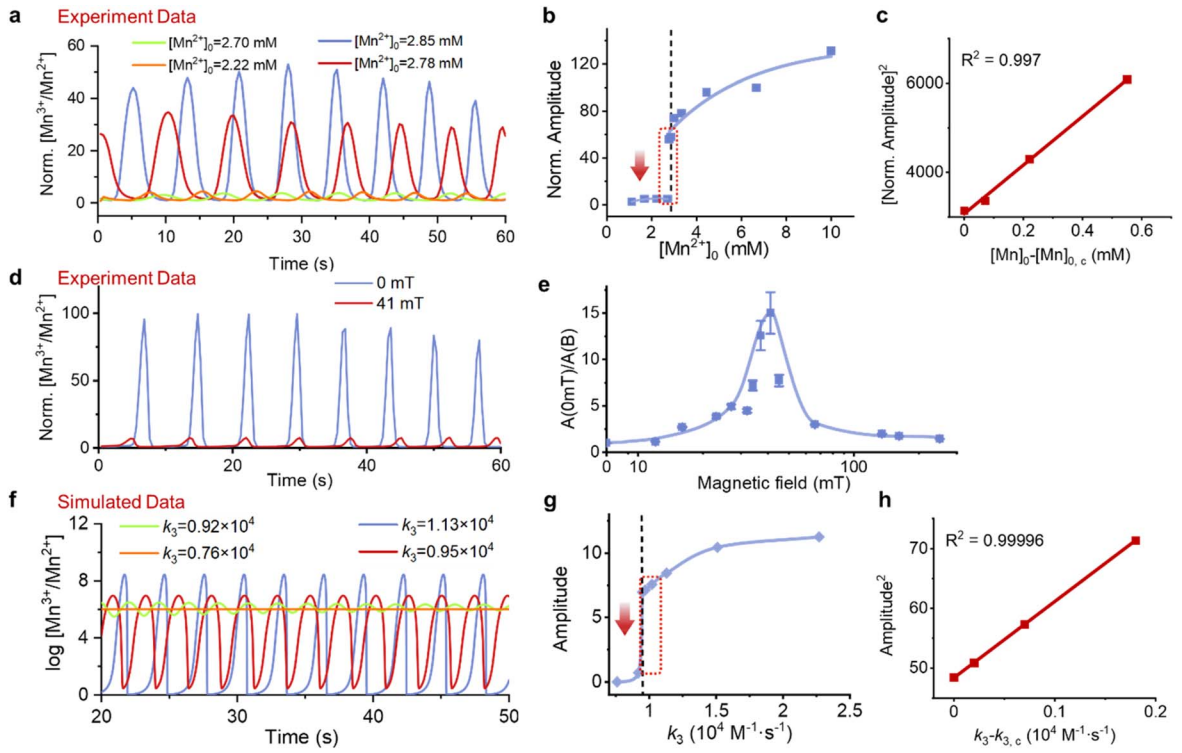

Fig. 3 Exploring the Hopf bifurcation point. (a) Normalized $[Mn^{3+}]/[Mn^{2+}]$ *versus* time measured for different initial $[Mn^{2+}]_0$. The amplitude of $[Mn^{3+}]/[Mn^{2+}]$ when $[Mn^{2+}]_0$ = 6.67 mM is defined as 100. (b) The dependence of the oscillation amplitude on $[Mn^{2+}]_0$. (c) The square of the oscillation amplitude as a function of ($[Mn^{2+}]_0 - [Mn^{2+}]_{0,c}$) where $[Mn^{2+}]_{0,c}$, represents the critical concentration as 2.78 mM. (d) Normalized $[Mn^{3+}]/[Mn^{2+}]$ *versus* time measured at 0 mT (blue line) and 41 mT (red line). The maximum amplitude at 0 mT is defined as 100. (e) The MF-dependence (0–250 mT) of the oscillation amplitude, *mfe*, defined here as $A(0)/A(B)$, where $A(B)$ is the average amplitude in the presence of a MF of intensity B. (f) Simulated time traces of normalized $\log([Mn^{3+}]/[Mn^{2+}])$ for different values of k_3. (g) Simulated dependence of the oscillation amplitude on k_3. (h) Square of the simulated oscillation amplitude as a function of ($k_3 - k_{3,c}$), where $k_{3,c}$ represents the critical k_3 value as 0.95 × 10^{-4} s^{-1}.

Open Access Article. Published on 08 September 2025. Downloaded on 06.02.26 19:00:58.
This article is licensed under a Creative Commons Attribution-NonCommercial 3.0 Unported Licence.

behavior that closely resembles a Hopf bifurcation, we specifically refer to it as a Hopf bifurcation. Our detailed analysis and experimental findings indicate that the Hopf bifurcation seems to occurs near $[Mn^{2+}]_0 = 2.78$ mM.

Next, we examined whether MFs perturb the oscillations close to the Hopf bifurcation, specifically at $[Mn^{2+}]_0 \approx 2.78$ mM. Increasing the applied MF from 0 to 41 mT led to a large (15-fold) decrease in the $[Mn^{3+}]/[Mn^{2+}]$ ratio (Fig. 3d and e) and a smaller (10%) decrease in the oscillation frequency, from 0.125 s^{-1} to 0.114 s^{-1}. At other $[Mn^{2+}]_0$ concentrations, the MFEs on the amplitudes were smaller than at 2.78 mM (Fig. S8). To summarize, from 0 to 41 mT, the *mfe* increased, reaching a maximum value of 15-fold, and then fell to 1.5-fold as the MF was changed from 41 to 250 mT (Fig. 3e and S9). Importantly, the conversion to products was only slightly affected by MFs, indicating that MFEs primarily influence the kinetics rather than the thermodynamics of the chemical oscillations.

We used the de Kepper–Epstein model to simulate the experimental results using Mathematica 12 (Fig. 3f, g and S10). By adjusting the magneto-sensitive rate constant k_3, we were able to induce the Hopf bifurcation. Since $[Mn^{2+}]$ remains relatively constant, we represented the changes in the $[Mn^{3+}]/[Mn^{2+}]$ ratio through $[Mn^{3+}]$ in our simulations. The $\log[Mn^{3+}]/[Mn^{2+}]$ oscillated between 0 and 11 when k_3 was within the range 0.75×10^4 to 2.27×10^4 M^{-1} s^{-1}, similar to the changes induced by variation of $[Mn^{2+}]_0$ shown in Fig. 3a. When we decreased k_3 from 2.27×10^4 to 0.95×10^4 M^{-1} s^{-1}, the amplitudes of oscillation fell from 11 to 7. However, further decreasing k_3 from 0.95×10^4 to 0.92×10^4 M^{-1} s^{-1} caused $\log[Mn^{3+}]$ to decrease 10-fold (Fig. 3f and g), comparable to the perturbation caused by either reducing $[Mn^{2+}]_0$ from 2.78 to 2.70 mM or applying a 41 mT MF. When $k_3 \gtrsim k_{3,c}$, the critical value of k_3 as 0.95×10^4 M^{-1} s^{-1}, the squared amplitude remains linearly proportional to $(k_3 - k_{3,c})$ (Fig. 3h), confirming this as a supercritical Hopf bifurcation, consistent with experimental results. This simulation demonstrates that oscillations near the Hopf bifurcation amplify the MFEs on the concentrations of the reaction intermediates. Player *et al.* and others have theoretically proposed such amplification based on the Brusselator model,[30,40] we have now observed it experimentally for the first time, underscoring the significance of the Hopf bifurcation for MF-sensitive chemical oscillations.

Tuning oscillations with a switched magnetic field

To confirm that the applied MF induces changes in the BR reaction, we conducted experiments with the MF switched on and off. As shown in Fig. 4a, applying a 41 mT MF resulted in a remarkable 13-fold decrease in the amplitude of oscillations to zero field. On removal of the MF, we observed a partial recovery in amplitude (Fig. S11a). Conversely, starting with a 41 mT MF and then switching it off led to a rapid 3.5-fold increase in amplitude (Fig. 4b and S11b). These results confirm that addition or removal of the applied MF greatly impacts the oscillator, particularly when near the Hopf bifurcation. Following the chemical amplification study by Kattnig *et al.*,[17] we used the prompt and delayed amplitudes to define the

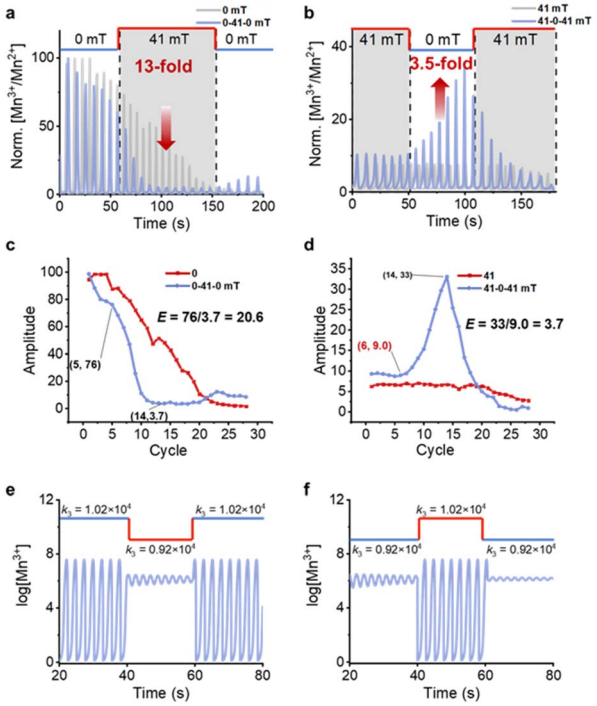

Fig. 4 Switched magnetic fields affect the BR oscillation. Time traces of normalized $[Mn^{3+}]/[Mn^{2+}]$ with off-on-off (a) and on-off-on (b) MF modes. respectively. The amplitude of the oscillations can be reversibly altered by changing the applied MF. The MF was 41 mT in the gray areas and 0 mT in the white areas. (c) Amplitude traces with cycle of off–on-(41 mT)-off and 0 mT. (d) Amplitude traces with cycle of on-(41 mT)-off-on-(41 mT) and 41 mT. (e and f) Simulated time traces of normalized $\log[Mn^{3+}]$ when small, sudden changes were made in the value of k_3: (e) $k_3 = 1.02 \times 10^4 \rightarrow 0.92 \times 10^4 \rightarrow 1.02 \times 10^4$ M^{-1} s^{-1} and (f) $k_3 = 0.92 \times 10^4 \rightarrow 1.02 \times 10^4 \rightarrow 0.92 \times 10^4$ M^{-1} s^{-1}.

amplification factor. As demonstrated in Fig. 4c and d, the application of a 41 mT resulted in a significant 20.6-fold decrease in amplitude compared to conditions with 0 mT. By contrast, starting with a 41 mT magnetic field and then turning it off led to a rapid 3.7-fold increase in amplitude.

We performed additional simulations to explore the dynamics of the changes in oscillation amplitude. In these calculations, we assumed that abrupt application of a 41 mT MF changed the rate constant k_3 from 1.02×10^4 to 0.92×10^4 M^{-1} s^{-1}. This change resulted in a sudden decline in amplitude from 7.5 to 0.75. When k_3 was switched back to 1.02×10^4 M^{-1} s^{-1}, the amplitudes returned to their former levels (Fig. 4e). In contrast, increasing k_3 from 0.92×10^4 to 1.02×10^4 M^{-1} s^{-1} produced a sudden increase in amplitude, which consistently reverted upon changing k_3 back to 0.92×10^4 M^{-1} s^{-1} (Fig. 4f). These results demonstrate that even weak MFs can disrupt stability, leading the system to transition between states at the Hopf bifurcation.

Magnetic field effect on the limit cycles

Iodide (I^-), another key intermediate in the BR reaction, can also exhibit nonlinear concentration changes (eqn (12)–(15)):

$$IO_3^- + I^- + 2H^+ \rightarrow HIO_2 + HIO \quad (12)$$

© 2025 The Author(s). Published by the Royal Society of Chemistry

Open Access Article. Published on 08 September 2025. Downloaded on 06.02.26 19:00:58.
This article is licensed under a Creative Commons Attribution-NonCommercial 3.0 Unported Licence.

$$HIO_2 + I^- + H^+ \rightarrow 2HIO \quad (13)$$

$$I^- + H^+ + HIO \rightarrow I_2 + H_2O \quad (14)$$

$$I_2 + MA \rightarrow IMA + I^- + H^+ \quad (15)$$

To establish the correlation between $[I^-]$ and the normalized concentration ratio $[Mn^{3+}]/[Mn^{2+}]$, we monitored $[I^-]$ using an iodide-selective electrode for different initial Mn^{2+} concentrations. When $[Mn^{2+}]_0$ was 3.00, 2.85, and 2.78 mM, the amplitude of the oscillations in $[I^-]$ remained stable, fluctuating between 0.9 $\times$ 10^{-8} and 1.1 $\times$ 10^{-8} M. However, when $[Mn^{2+}]_0$ was further lowered to 2.70 mM, there was a substantial drop in the amplitude of $[I^-]$ oscillations, to 1.0 $\times$ 10^{-9} M, which persisted when $[Mn^{2+}]_0$ was further decreased to 2.22 mM (Fig. 5a, b and S12a). The reduction in $[Mn^{2+}]_0$ from 2.78 mM to 2.70 mM resulted in a 9-fold decrease in the amplitude of $[I^-]$, which correlates with the amplitude change for $[Mn^{3+}]$ observed at the Hopf bifurcation.

During this investigation, we measured the *mfe* of $[I^-]$. At a MF strength of 41 mT, the amplitude of $[I^-]$ oscillations decreased by a factor of 5 compared to zero field, clearly demonstrating that $[I^-]$ is sensitive to MFs when $[Mn^{2+}]_0$ = 2.78 mM, as illustrated in Fig. 5c and S12b. Importantly, the phase of the $[I^-]$ oscillations was opposite to that of $[Mn^{3+}]$, indicating that $[I^-]$ acts as a reduced species while $[Mn^{3+}]$ operates as an oxidized species (Fig. S13). Therefore, the range of limit cycle oscillations in $[I^-]$ and in the normalized $[Mn^{3+}/Mn^{2+}]$ ratio is between 6 $\times$ 10^{-9} and 1.2 $\times$ 10^{-8} M, and between 0 to 100, respectively. After applying a 41 mT MF, the oscillation ranges for $[I^-]$ and normalized $[Mn^{3+}]/[Mn^{2+}]$ changed to 3.4 $\times$ 10^{-9} to 5.5 $\times$ 10^{-8} M, and 0 to 7, respectively, resulting in approximately 5- and 15-fold decreases, respectively, in the two amplitudes (Fig. 5d). Such changes lead to a significant contraction in the shape and size of the limit cycle.

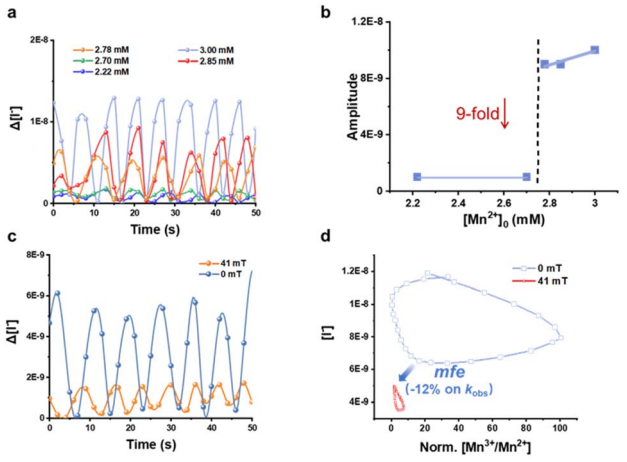

Fig. 5 Iodide concentration and limit cycle. (a) Time traces of $\Delta[I^-]$ at different $[Mn^{2+}]_0$ (ranging from 2.22 mM to 3.00 mM), $\Delta[I^-]$ is defined as the difference between the real-time concentration and the minimum concentration. (b) The dependence of the oscillation amplitude on $[Mn^{2+}]_0$. (c) Time traces of $\Delta[I^-]$ in 0 mT (blue line) and 41 mT (orange line) MFs. (d) Oscillations of $[I^-]$ and normalized $[Mn^{3+}]/[Mn^{2+}]$ represented as a limit cycle at 0 mT (blue line) and 41 mT (red line). The concentration of I^- was measured using an iodide ion-selective electrode.

Thus, these results further demonstrate that both $[I^-]$ and $[Mn^{3+}]$ intermediates exhibit considerable amplification near the Hopf bifurcation, even though the MFEs on the individual reactions are minor.

The proposed mechanism related to radical pair mechanism

In the fields of biology and chemistry, MFEs have been well-established and are plausibly attributed to the spin dynamics of transient radical pairs according to the radical pair mechanism (RPM).[5,21,42] However, when considering magnetic fields with weaker interaction energies (approximately 10^{-2} kJ mol^{-1} T^{-1}), the observed changes in reaction rates and product yields are typically small—often less than a few percent. In spite of extensive research,[43] there has been no conclusive evidence to show that a magnetic field as weak as Earth's can induce measurable alterations in the rates of chemical reactions or the yields of their products.[44] Nonetheless, previous studies have shown that weak MFs can effectively influence biological oscillatory processes, such as circadian rhythms.[7,45] Using the Brusselator model oscillator,40 the intermediate concentrations can be extraordinarily sensitive to minor changes near the Hopf bifurcation, forming a chemical basis for amplifying MFEs in oscillatory processes.

Based on previous works,[30,40] we also propose that MFEs could arise at the autocatalysis step *via* a radical pair driven by HIO_2 autocatalysis.[38,45] Thus, we suggest that single-electron transfer from I^- to HIO produces the singlet RP $[I^\bullet\ {}^\bullet IOH^-]$ that can recombine to generate I_2 and enable the reaction to progress (eqn (11)). The singlet RP can undergo reverse electron transfer to regenerate I_2, while the triplet spin state is unreactive, resulting in the formation of free $I^\bullet$ radicals. We tentatively suggest that the sharp decrease and recovery of the MFE in Fig. 1c emerges from a change in singlet-triplet mixing due to a "2J-resonance" (Fig. S14–S17, S18b and S19). However, the BR system involves several reactive species and radicals, including Mn^{2+}, Mn^{3+}, and $I^\bullet$, adding complexity to our understanding of the mechanisms by which MFs influence autocatalysis (details in SI Section 10).

$$I^- + HIO \rightarrow [I^\bullet\ {}^\bullet IOH^-] \rightarrow I_2 + H_2O \quad (16)$$

Meanwhile, to further investigate the MF-responsive species, we conducted experiments using Ce^{3+} ($Ce(NO_3)_3$, 0.0067 M). Interestingly, by monitoring the open-circuit potential-time profiles, we observed that at 41 and 200 mT, k_{obs} decreased by 4.3% and 6.1% respectively (Fig. S20). The MFEs are comparable to those found in the Mn^{2+} systems (Fig. 1c). This finding not only provides further validation for the radical pair mechanism of the reaction, but also suggests that the MFEs are not limited to a specific catalyst ion, and iodine-centered radicals serve as the primary magneto-responsive species in this system. The divergence in MFE magnitudes likely stems from variations in radical-pair lifetimes and associated electron-transfer kinetics induced by different metal ion catalyst. This observation opens up new avenues for future research to explore the underlying principles and potential applications of such MFEs in chemical reactions. Future studies could focus on investigating the detailed mechanisms of how different catalyst ions influence the radical pair

Open Access Article. Published on 08 September 2025. Downloaded on 06.02.26 19:00:58. This article is licensed under a Creative Commons Attribution-NonCommercial 3.0 Unported Licence.

dynamics and the resulting magnetic field effects, as well as exploring the possibility of using other types of catalysts or reaction systems to achieve similar or even enhanced effects.

Conclusions

This study demonstrates that weak MFs can exert profound control over chemical oscillators when the system operates near a critical threshold known as the Hopf bifurcation. By applying MFs (0–200 mT) to the BR reaction, we observed a 12% enhancement in reaction rate while 1500% enhancement in oscillation amplitudes of key intermediates (Mn^{2+} and I^-), far exceeding previously reported effects in feedback-driven chemical systems. This phenomenon arises from the inherent nonlinear sensitivity of systems near bifurcation points, where even minor perturbations such as MF-induced changes in spin-selective radical recombination rates are amplified, driving macroscopic transitions from steady states to sustained oscillations.

Mechanistically, magnetic fields alter the spin dynamics of radical pairs, shifting their recombination efficiency and affecting reaction kinetics. Simulations using the de Kepper–Epstein model confirm that such subtle kinetic changes can destabilize steady states and dramatically amplify oscillatory behavior. These findings highlight the critical role of proximity to bifurcation points in governing system responsiveness, similar to phase transitions in physical systems.

The implications of this research extend beyond oscillatory chemistry, providing a framework for exploiting critical dynamics in magnetically tunable systems. Furthermore, this work bridges nonlinear dynamics and magnetochemistry, suggesting that weak environmental fields often dismissed as inconsequential could play significant roles in biological rhythms or material science. Future research should investigate the effects of MFs in various oscillatory systems (*e.g.*, biological clocks) and refine theoretical frameworks to exploit bifurcation-sensitive control. Ultimately, this study highlights the potential of critical-point engineering to unlock extraordinary responsiveness to external stimuli, paving the way for innovations at the intersection of chemistry, physics, and biology.

Author contributions

J.-L. Z. initiated and conceptualized the research project. S. Z. conducted all experimental investigations and computational analyses. Z.-S. Y. and S. Z. worked together to design and optimize the experimental protocols, with S. Z. also responsible for data inspection and interpretation. B.-W. W., S. G., and J.-L. Z. contributed to project administration and funding coordination. S. Z. drafted the manuscript, which underwent critical revisions and received intellectual input and final approval from all co-authors.

Conflicts of interest

The authors declare no competing financial interests.

Data availability

Data for this article, including experimental procedure, supplementary tables and figures, calculation details, *etc.* are available in the SI. A supplementary movie recording the oscillations is attached. See DOI: **https://doi.org/10.1039/d5sc05941k**.

Acknowledgements

We acknowledge financial support from the National Natural Science Foundation of China (22131003, 22488101 and 22401014). We acknowledge the Analytical Instrumentation Center of Peking University. We thank Prof. P. J. Hore from Oxford University for kind discussion and revisions.

References

1 V. L. Bliss and F. H. Heppner, Circadian activity rhythm influenced by near zero magnetic field, *Nature*, 1976, **261**, 411–412.
2 P. J. Hore, Are biochemical reactions affected by weak magnetic fields?, *Proc. Natl. Acad. Sci. U. S. A.*, 2012, **109**, 1357–1358.
3 Z.-S. Yang, S. Gao and J.-L. Zhang, Magnetic manipulation of the reactivity of singlet oxygen: from test tubes to living cells, *Natl. Sci. Rev.*, 2024, nwae069.
4 J.-L. Sessler, Achieving magnetic control of cellular events by introducing non-native radical pair formation, *Natl. Sci. Rev.*, 2024, nwae145.
5 U. E. Steiner and T. Ulrich, Magnetic field effects in chemical kinetics and related phenomena, *Chem. Rev.*, 1989, **89**, 51–147.
6 A. C. Møller and L. F. Olsen, Effect of magnetic fields on an oscillating enzyme reaction, *J. Am. Chem. Soc.*, 1999, **121**, 6351–6354.
7 A. F. Taylor, M. R. Tinsley, F. Wang, Z. Huang and K. Showalter, Dynamical quorum sensing and synchronization in large populations of chemical oscillators, *Science*, 2009, **323**, 614–617.
8 L. F. Olsen and H. Degn, Chaos in biological systems, *Q. Rev. Biophys.*, 1985, **18**, 165–225.
9 C. S. Colwell, Linking neural activity and molecular oscillations in the SCN, *Nat. Rev. Neurosci.*, 2011, **12**, 553–569.
10 R. J. Field and R. M. Noyes, Oscillations in chemical systems. V. Quantitative explanation of band migration in the Belousov-Zhabotinskii reaction, *J. Am. Chem. Soc.*, 1974, **96**, 2001–2006.
11 S. D. Furrow and R. M. Noyes, The oscillatory Briggs-Rauscher reaction. 1. Examination of subsystems, *J. Am. Chem. Soc.*, 1982, **104**, 38–42.
12 A. M. Zhabotinsky, A history of chemical oscillations and waves, *Chaos*, 1991, **1**, 379–386.
13 R. E. Dolmetsch, K. Xu and R. S. Lewis, Calcium oscillations increase the efficiency and specificity of gene expression, *Nature*, 1998, **392**, 933–936.

© 2025 The Author(s). Published by the Royal Society of Chemistry

Open Access Article. Published on 08 September 2025. Downloaded on 06.02.26 19:00:58. This article is licensed under a Creative Commons Attribution-NonCommercial 3.0 Unported Licence.

14 M. G. Howlett, A. H. J. Engwerda, R. J. H. Scanes and S. P. Fletcher, An autonomously oscillating supramolecular self-replicator, *Nat. Chem.*, 2022, **14**, 805–810.
15 H. Zhang, H. Zeng, A. Eklund, H. Guo, A. Priimagi and O. Ikkala, Feedback-controlled hydrogels with homeostatic oscillations and dissipative signal transduction, *Nat. Nanotechnol.*, 2022, **17**, 1303–1310.
16 M. ter Harmsel, O. R. Maguire, S. A. Runikhina, A. S. Y. Wong, W. T. S. Huck and S. R. Harutyunyan, A catalytically active oscillator made from small organic molecules, *Nature*, 2023, **621**, 87–93.
17 D. R. Kattnig, E. W. Evans, V. Déjean, C. A. Dodson, M. I. Wallace, S. R. Mackenzie, C. R. Timmel and P. J. Hore, Chemical amplification of magnetic field effects relevant to avian magnetoreception, *Nat. Chem.*, 2016, **8**, 384–391.
18 D. R. Kattnig and P. J. Hore, The sensitivity of a radical pair compass magnetoreceptor can be significantly amplified by radical scavengers, *Sci. Rep.*, 2017, **7**, 11640.
19 H. Mouritsen, Long-distance navigation and magnetoreception in migratory animals, *Nature*, 2018, **558**, 50–59.
20 P. J. Hore, Upper bound on the biological effects of 50/60 Hz magnetic fields mediated by radical pairs, *eLife*, 2019, **8**, e44179.
21 C. Eichwald and J. Walleczek, Model for magnetic field effects on radical pair recombination in enzyme kinetics, *Biophys. J.*, 1996, **71**, 623–631.
22 A. Christine Møller, A. Lunding and L. Folke Olsen, Further studies of the effect of magnetic fields on the oscillating peroxidase–oxidase reaction, *Phys. Chem. Chem. Phys.*, 2000, **2**, 3443–3446.
23 E. Boga, S. Kádár, G. Peintler and I. Nagypál, Effect of magnetic fields on a propagating reaction front, *Nature*, 1990, **347**, 749–751.
24 X. He, K. Kustin, I. Nagypal and G. Peintler, A family of magnetic field dependent chemical waves, *Inorg. Chem.*, 1994, **33**, 2077–2078.
25 R. Evans, C. R. Timmel, P. J. Hore and M. M. Britton, Magnetic resonance imaging of a magnetic field-dependent chemical wave, *Chem. Phys. Lett.*, 2004, **397**, 67–72.
26 R. Evans, C. R. Timmel, P. J. Hore and M. M. Britton, Magnetic resonance imaging of the manipulation of a chemical wave using an inhomogeneous magnetic field, *J. Am. Chem. Soc.*, 2006, **128**, 7309–7314.
27 H. Okano, H. Kitahata, D. Akai and N. Tomita, The Influence of a gradient static magnetic field on an unstirred Belousov–Zhabotinsky reaction, *Bioelectromagnetics*, 2008, **29**, 598–604.
28 H. Okano, H. Kitahata and D. Akai, Effect of a gradient static magnetic field on an unstirred Belousov–Zhabotinsky reaction by changing the thickness of the medium, *J. Phys. Chem. A*, 2009, **113**, 3061–3067.
29 R. Nishikiori, S. Morimoto, Y. Fujiwara, A. Katsuki, R. Morgunov and Y. Tanimoto, Magnetic field effect on chemical wave propagation from the Belousov–Zhabotinsky reaction, *J. Phys. Chem. A*, 2011, **115**, 4592–4597.
30 T. C. Player, E. D. A. Baxter, S. Allatt and P. J. Hore, Amplification of weak magnetic field effects on oscillating reactions, *Sci. Rep.*, 2021, **11**, 9615.
31 K. E. M. Church, and X. Liu, in *Bifurcation Theory of Impulsive Dynamical Systems*, ed. Church, K. E. M., and Liu, X., Springer International Publishing, Cham, 2021, pp. 235–249.
32 I. Millett, W. Vance and J. Ross, Measurements of phase response in an oscillatory reaction and deduction of components of the adjoint eigenvector, *J. Phys. Chem. A*, 1999, **103**, 8252–8256.
33 M. Broens and K. Bar-Eli, Canard explosion and excitation in a model of the Belousov-Zhabotinskii reaction, *J. Phys. Chem.*, 1991, **95**, 8706–8713.
34 B.-W. Qin, K.-W. Chung, A. Algaba and A. J. Rodríguez-Luis, High-order analysis of canard explosion in the Brusselator equations, *Int. J. Bifurcat. Chaos*, 2020, **30**, 2050078.
35 A. C. Møller and L. F. Olsen, Perturbations of simple oscillations and complex dynamics in the peroxidase–oxidase reaction using magnetic fields, *J. Phys. Chem. B*, 2000, **104**, 140–146.
36 O. R. Maguire, A. S. Y. Wong, J. H. Westerdiep and W. T. S. Huck, Early warning signals in chemical reaction networks, *Chem. Commun.*, 2020, **56**, 3725–3728.
37 S. D. Furrow and R. M. Noyes, The oscillatory Briggs-Rauscher reaction. 2. Effects of substitutions and additions, *J. Am. Chem. Soc.*, 1982, **104**, 42–45.
38 R. M. Noyes and S. D. Furrow, The oscillatory Briggs-Rauscher reaction. 3. A skeleton mechanism for oscillations, *J. Am. Chem. Soc.*, 1982, **104**, 45–48.
39 R. J. Field, E. Koros and R. M. Noyes, Oscillations in chemical systems. II. Thorough analysis of temporal oscillation in the bromate-cerium-malonic acid system, *J. Am. Chem. Soc.*, 1972, **94**, 8649–8664.
40 P. A. Purtov, External magnetic fields as a possible cause of stability disturbance of stationary states far from equilibrium in reactions involving radical pairs, *Appl. Magn. Reson.*, 2004, **26**, 83–97.
41 J. E. Marsden; M. McCracken; S. New; Y. Berlin, 1976.
42 C. T. Rodgers, Magnetic field effects in chemical systems, *Pure Appl. Chem.*, 2009, **81**, 19–43.
43 B. Brocklehurst, Magnetic fields and radical reactions: recent developments and their role in nature, *Chem. Soc. Rev.*, 2002, **31**, 301–311.
44 J. Walleczek, in *Electricity and Magnetism in Biology and Medicine*, ed. Bersani, F., Springer US, Boston, MA, 1999, pp. 363–366.
45 P. De Kepper and I. R. Epstein, Mechanistic study of oscillations and bistability in the Briggs-Rauscher reaction, *J. Am. Chem. Soc.*, 1982, **104**, 49–55.